
This is an electronic reprint of the original article.
This reprint may differ from the original in pagination and typographic detail.

Ramesh, Raju; Arivazhagan, Ponnusamy; Prabakaran, K.; Sanjay, S.; Baskar, K.

Influence of AlN interlayer on AlGaN/GaN heterostructures grown by metal organic chemical vapour deposition

Published in:
Materials Chemistry and Physics

DOI:
[10.1016/j.matchemphys.2020.124003](https://doi.org/10.1016/j.matchemphys.2020.124003)

Published: 01/02/2021

Document Version
Peer-reviewed accepted author manuscript, also known as Final accepted manuscript or Post-print

Published under the following license:
CC BY-NC-ND

Please cite the original version:
Ramesh, R., Arivazhagan, P., Prabakaran, K., Sanjay, S., & Baskar, K. (2021). Influence of AlN interlayer on AlGaN/GaN heterostructures grown by metal organic chemical vapour deposition. *Materials Chemistry and Physics*, 259, Article 124003. <https://doi.org/10.1016/j.matchemphys.2020.124003>

This material is protected by copyright and other intellectual property rights, and duplication or sale of all or part of any of the repository collections is not permitted, except that material may be duplicated by you for your research use or educational purposes in electronic or print form. You must obtain permission for any other use. Electronic or print copies may not be offered, whether for sale or otherwise to anyone who is not an authorised user.

Influence of AlN interlayer on AlGaN/GaN Heterostructures grown by metal organic chemical vapour deposition

R. Ramesh^{1,*}, P. Arivazhagan², K.Prabakaran³, S. Sanjay⁴, K. Baskar⁵

¹Department of Electronics and Nanoengineering, Aalto University, P O BOX 13500, FI-00076, Finland

²Nano-Functional Materials Technology Centre (NFMTC), Department of Metallurgical & Materials Engineering, Indian Institute of Technology, Chennai 600 036, Tamilnadu, India

³ Key Laboratory for Micro-Nano Physics and Technology of Hunan Province, College of Materials Science and Engineering, Hunan University, Changsha 410082, P.R China

⁴Department of Electronics and Communication Engineering, Koneru Lakshmaiah Education Foundation, Hyderabad, 500 075, Telangana, India

⁵Crystal Growth Centre, Anna University, Chennai 600 025, India

***Corresponding Author:**

Dr. R. Ramesh

Staff Scientist

Department of Electronics and Nanoengineering

Aalto University,

Tietotie 3, Espoo Finland

E-Mail: ramesh.raju@aalto.fi (R. Ramesh)

Abstract

AlGa_N/Ga_N heterostructures with different thicknesses of AlN interlayer (AlN-IL) were grown by metal organic chemical vapour deposition (MOCVD) system. The results obtained from atomic force microscopy revealed that, surface roughness decreases with increase in the interlayer thickness. Scanning electron microscopy and transmission electron microscopy images portrayed good interfaces between AlGa_N/Ga_N heterostructures containing AlN as the IL. From the high-resolution X-ray diffraction data, the aluminium composition was estimated as 21-24%, and the AlGa_N layer thicknesses were found to be 22-26 nm in the AlGa_N layers using the epitaxy smooth fit software. Using reciprocal space mapping, the strain between AlGa_N and Ga_N layers scanned along (1 0 5) plane were analyzed for the AlGa_N/Ga_N heterostructures. Photoluminescence (PL) spectroscopy revealed a significant shift in the AlGa_N peaks for samples both in the presence and absence of AlN-IL. Time resolved photoluminescence results exhibit dominate decay time in AlGa_N/Ga_N heterostructures samples containing AlN-IL of around 3 ns thick. It is to be noted that, mobility increased from 1246 to 2000 cm²/volt-sec due to the presence of AlN-IL at 300 K.

Keywords: MOCVD, AlGa_N, AlN Interlayer, Atomic Force Microscopy, Hall Measurement, Time Resolved Photoluminescence;

1. Introduction

Over the past few decades, gallium nitride (GaN) and aluminium gallium nitride (AlGaN) based heterostructures for high-electron mobility transistors (HEMT) have received inevitable consideration due to their potential for high power and high-frequency applications [1,2]. This is because, nitride-based devices possess fascinating properties such as wide energy bandgap, high critical breakdown electric field (3 MV/cm) and high electron saturation velocity compared with that of the conventional silicon or GaAs devices [3-6]. In addition, AlGaN is extensively preferred in the applications such as ultraviolet (UV) light emitting diodes, UV photodetectors and chemical sensors [7, 8]. The fascinating property about AlGaN and GaN combo is the formation of two-dimensional electron gas (2DEG) at the interface due to strong spontaneous and piezoelectric polarization. As a result, high electron concentration ($> 1 \times 10^{13} \text{ cm}^{-2}$) and mobility [1000–2000 $\text{cm}^2/(\text{Vs})$] can be attained without doping by metal organic chemical vapour deposition (MOCVD) [9]. However, the mobility of electrons suffers due to the lattice stress, dislocations, interface roughness and alloy disorder scattering [10]. These problems can be overcome by utilizing a thin layer of aluminium nitride (AlN) as Interlayer (IL) improves the heterostructure interface quality as well as reduces dislocations and alloy disorders during the growth of AlGaN-based HEMT heterostructures. And also, AlN-IL acts as a barrier by minimizing the charge carrier tunneling [5, 9, 11-17]. Based on earlier reports, we have reported a better quality AlGaN layers grown on GaN/sapphire templates using MOCVD [18-20]. The present work focuses on considerable improvements in the structural, morphological and optical properties of AlGaN/GaN heterostructures containing a thin AlN interlayer. Temperature dependent Hall Effect properties and related scattering mechanisms, luminescence decay time in AlGaN/GaN HEMT structures were investigated.

2. Experimental Details

The AlGa_N/Ga_N heterostructures with and without AlN-IL were grown on c-sapphire substrates using MOCVD (Aixtron 200/4/RF-S). Trimethylgallium (TMGa), Trimethyl aluminium (TMAI) and Ammonia (NH₃) were used as the precursors for Ga, Al and N. Hydrogen (H₂) was used as the carrier gas. Prior to the growth, c-plane sapphire (miscut of 0.2°) was thermally annealed at 1050°C for 10 min under H₂ ambience to remove the native oxides present on the substrates. A 30 nm thick low temperature Ga_N nucleation layer was grown at 500°C with a V/III ratio of 3350, followed by growth of 1.8 μm Ga_N grown at 1020°C with a V/III ratio of 600. Then, AlN-IL was grown at 1040°C by varying the time as 10, 20, and 30 sec. Finally, AlGa_N layer was also grown at same temperature (1040°C), pressure (50 mbar), growth time (60 s), NH₃ flow (1300 standard cubic centimeter (sccm)) and TMAI flow (35 sccm) and TMGa flow (9 sccm) respectively for all the samples. The AlGa_N/Ga_N heterostructures grown without AlN-IL is named as sample I, while the AlN interlayer with thickness 1, 2 and 3 nm are named as samples II, III and IV respectively. The schematic representing AlGa_N/Ga_N heterostructures with and without AlN-IL is shown in Figure 1.

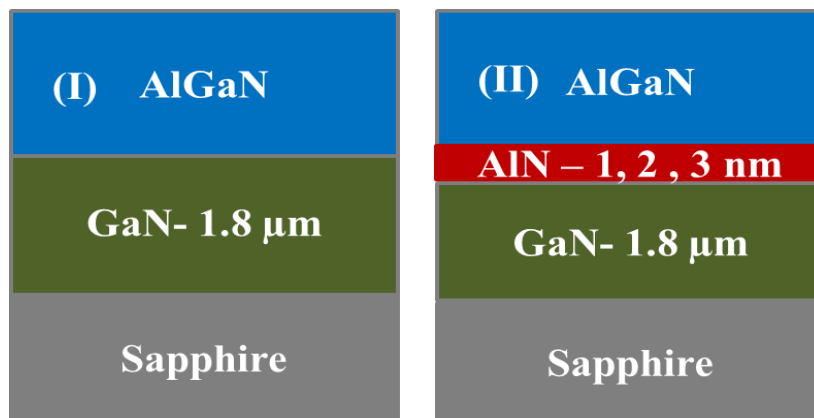


Figure 1. Schematic cross sectional view of (I) AlGa_N/Ga_N heterostructures
(II) AlGa_N/Ga_N heterostructures with AlN-IL (1-3 nm)

The surface morphology of AlGa_N layer was studied using atomic force microscopy [(AFM), Park XE100 with a curvature of cantilever tip <10 nm, the vertical and lateral resolution of the position sensitive photo detector as 0.1 nm and 30 nm). The crystalline quality, Al composition and thickness of the samples have been analyzed using high-resolution x-ray diffraction (HRXRD), [PANalytical X'Pert Pro MRD with a resolution of 0.0001/0.36 arcsec, Ge-(220) monochromator with Triple (Xe) axis and pixel detector]. High-resolution transmission electron microscopy [(HR-TEM), FEI, LaB₆ filament, accelerating voltage –300 KV with a point to point resolution of 0.2 nm] and scanning electron microscopy [(SEM), Carl Zeiss EVO 18, LaB₆ filament, accelerating voltage - 10 kV with secondary electron detector and point to point resolution of 10 nm) were used to verify the cross sections of heterostructures. The luminescence properties of the samples were examined using a photoluminescence (PL) spectrometer [Spectra-Physics with a Resolution of ±0.1 nm] with an excitation wavelength of 244 nm. The decay time measurements were carried out using time resolved photoluminescence (TRPL) spectrometer using an Nd:YAG laser with a pulse width of 100 fs and excitation wavelength of 266 nm at RT. The electrical properties of AlGa_N/Ga_N heterostructures were studied using the [ECOPIA HMS 5000] temperature dependent (80-350 ± 0.5K) Hall measurement system.

3. Results and discussions

3.1 Surface Analysis

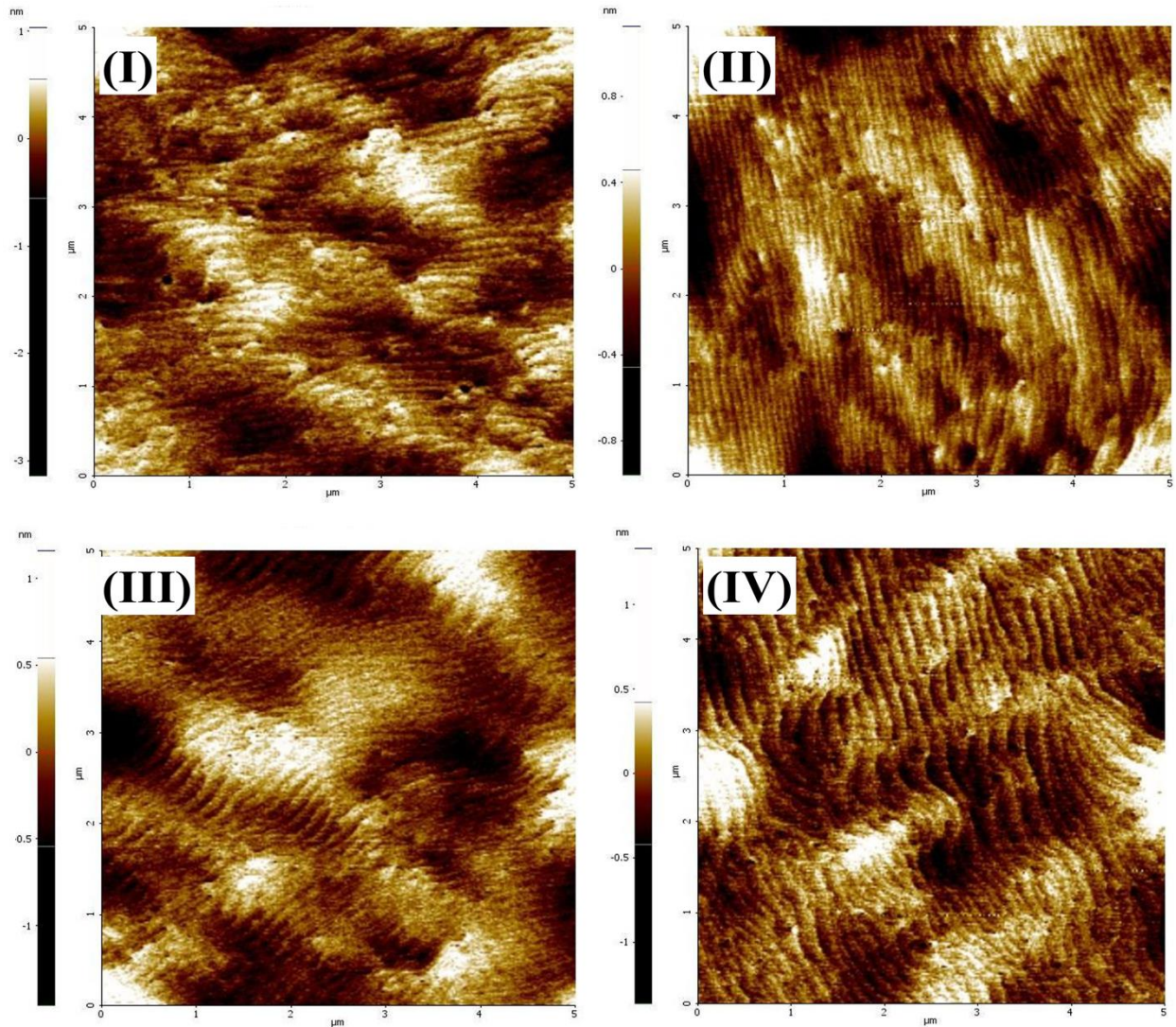


Figure 2. AFM ($5\mu\text{m}^2$) images of AlGaIn/GaN heterostructures with samples (I) without AlN-IL (II-IV) AlN-IL (1 - 3 nm)

The AFM test results in respect of AlGaIn/GaN heterostructures with and without AlN-IL are showcased in Figure 2. Their corresponding 3D images are shown in figure S1. The root mean square (rms) roughness of the samples were 0.245 (sample I), 0.231 (sample II), 0.194 (sample III), and 0.170 nm (sample IV) respectively. All the images obtained from AFM

showcased crack-free and atomically-flat surfaces with terrace step morphologies. Due to the lattice differences, pure or partial screw type dislocations (in the GaN layers) and randomly distributed V pits (in the AlGaN layers) were observed in all the samples [21]. The morphology is generally associated with the adatoms diffusing on the surface. As the diffusion length of Al atoms are smaller when compared to that of the Ga atoms, the Al atoms gets trapped at the interstitial sites and not at to the lattice position. As reported in the literature [22], with increase in the Al composition, both the V-pit density and surface disorder increased. However, when the thickness of the AlN-IL is increased, the surface quality of the AlGaN layers was found to get improved, as it tends to overcome the lattice differences. The obtained AFM images results clearly portrays that, AlN-IL with 3 nm thickness (sample IV) improved the surface morphology to nearly equal spaced terrace steps of AlGaN/GaN heterostructures when compared to that of the AlGaN/GaN heterostructures without AlN-IL of AlGaN/GaN heterostructures. Hence, it is concluded that interface roughness scattering mechanisms can be approached through surface roughness of AlGaN layers [12]. Therefore, the terrace step morphologies are helpful for the high performance HEMT applications [23]. Similar kind of morphologies have been observed by Hu et. al and Perozek et. al [14, 24].

3.2 Structural Analysis

The ω - 2θ scan were carried out using HRXRD in respect of AlGaN/GaN heterostructures with and without AlN-IL and are shown in Figure 3. From the results obtained, the composition and thickness of the samples were determined based on the Vegard's law [25]. The experimental data were fitted using the epitaxy smoothfit software. From figure 3, the high intensity GaN peak corresponds to a (0 0 2) diffraction pattern. The sample containing 3 nm AlN-IL layer (sample

IV) exhibit broad peak with good interface quality than the AlGa_N/Ga_N heterostructures without AlN-IL.

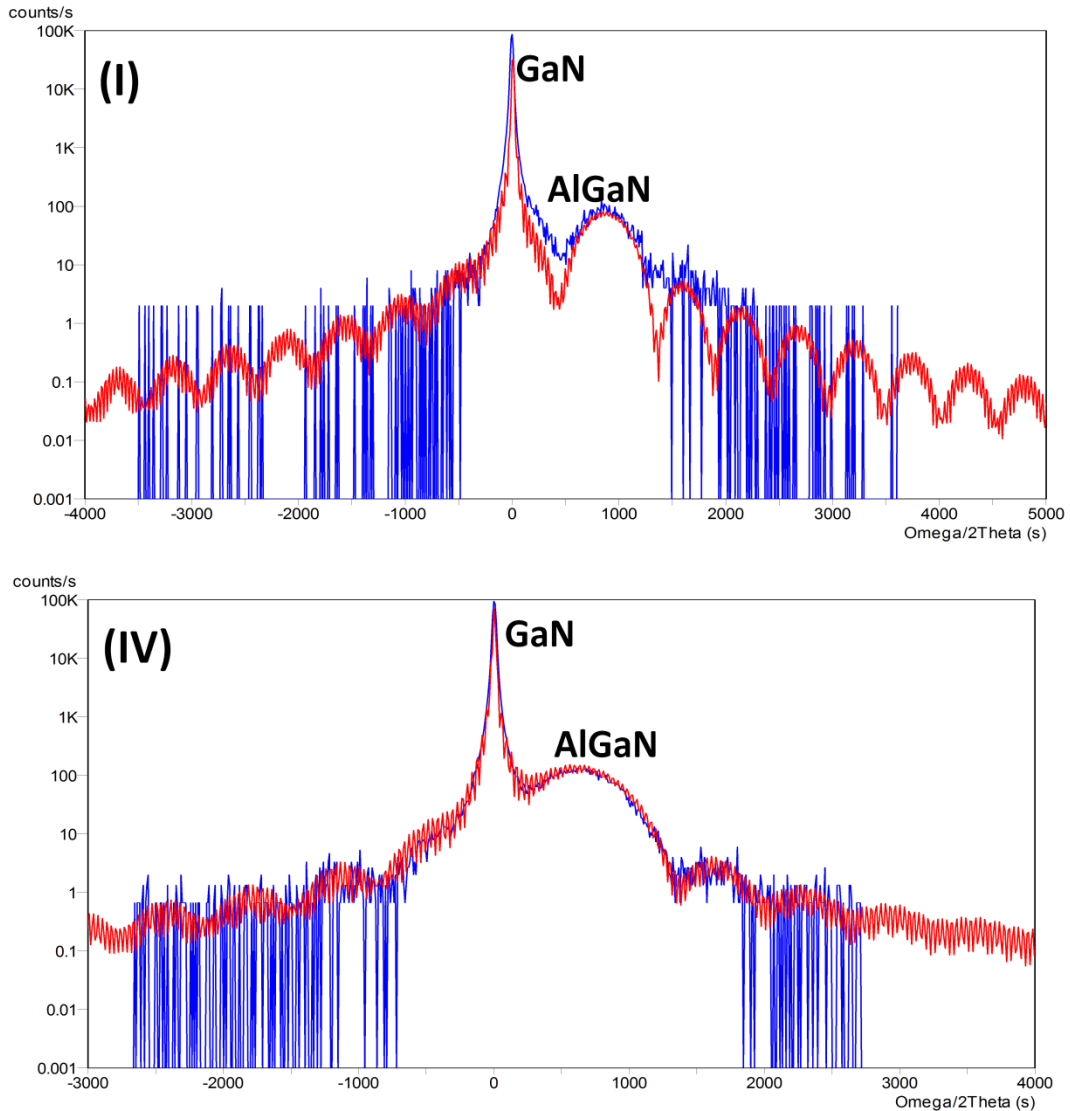


Figure 3. HRXRD (0 0 2) ω - 2θ scan of an AlGa_N/Ga_N heterostructures without and with AlN-IL (sample I, and IV) (Blue Line) along with Simulation (Red line)

By fitting for the diffraction pattern, the layer thickness (AlGa_N and AlN) and aluminium compositions (Al) were determined and are tabulated in Table 1. From table 1, the AlGa_N layer thickness has been found to decrease by increasing the AlN-IL thickness due to the parasitic

reaction of TMAI and NH₃ in the vapor phase [18]. In addition, sample I and II revealed almost similar Al composition as the 1 nm AlN-IL did not have much effect while grown via high temperature route. Whereas, in the case of 3 nm-AlN-IL (sample IV), higher amount of Al gets diffused into AlGa_N layer due to the high temperature effect. The cross-sectional SEM and HR-TEM analysis are shown in Figure S2.

Table 1 Structural Properties of AlGa_N/Ga_N heterostructures with and without AlN-IL

Samples	AlN-IL thickness	Al Composition (± 1 %)	AlGa_N thickness (± 2 nm)
I	No-IL	21	26
II	1 nm	21.5	26
III	2 nm	23	24
IV	3 nm	24	22

Furthermore, the crystalline quality of Ga_N layers were characterized by X-ray rocking curves (XRC) analysis along symmetric (0 0 2) and asymmetric (1 0 2) axis [27]. The FWHM values for (0 0 2) plane of Ga_N were 429, 387, 380 and 373 arc-sec, while for (1 0 2) plane were 416, 533, 632 and 672 arc-sec for samples I-IV respectively. It is worth noting that, the FWHM values of the (0 0 2) plane for sample I are higher than that of sample IV, whereas the (1 0 2) plane values of sample I are lower than the sample IV. These results reveal that tilt and twist misorientations are associated with the screw and edge threading dislocations (TDs) in Ga_N layers. On the other hand, sample IV revealed narrower FWHM values revealing better

crystalline quality. Approximate TDs ($D_{TD} = D_{screw} + D_{edge}$) is estimated using the following equations [26, 27],

$$D_{screw} = \frac{\alpha_{(002)}^2}{4.35|b_{screw}|^2} \quad D_{edge} = \frac{\beta_{(102)}^2}{4.35|b_{edge}|^2} \quad (1)$$

Where D_{screw} is screw dislocation density, D_{edge} is edge dislocation density, α (tilt) and β (twist) are the Full Width Half Maximum (FWHM) measured from (0 0 2) and (1 0 2) diffraction planes and b is the Burger vector length of dislocation ($b_{screw} = 0.5186$ nm, $b_{edge} = 0.3189$ nm). The screw dislocation density was calculated at 3.69×10^8 , 3×10^8 , 2.9×10^8 and 2.79×10^8 cm⁻² for samples I-IV, respectively. The edge dislocation density were determined at 9.2×10^8 , 1.50×10^9 , 2.12×10^9 and 2.40×10^9 cm⁻² for samples I-IV, respectively. In this context, edge TDs are the major contribution in all the samples, and higher than that of screw dislocations. It reveals that comparable good quality of the GaN epilayer [28]. Additionally, estimated screw TDs densities of the samples showed consistency in step growth were atomically flat in AFM images [24].

Figure 5 shows the (1 0 5) plane of asymmetric Reciprocal Space Mapping (RSM) in respect of AlGa_xN/GaN heterostructures with and without AlN-IL. Using the epitaxy smooth fit software, the reciprocal lattice point (RLP) coordinates of Q_x values was found to be 0.278490, 0.278481, 0.279137, and 0.278431 rlu for the GaN and top AlGa_xN layers (sample I-IV) in same direction. The GaN, AlGa_xN layer and AlN-IL sample contour shapes represent coherently strained AlGa_xN/GaN heterostructures. It is evident that for all samples, the AlGa_xN peaks vertically aligned with the GaN layer. This indicates that, the grown AlGa_xN epilayers (in-plane lattice constants) are pseudomorphic with the underlying GaN. There are no substantial variations in the AlGa_xN and AlN-IL peaks because of the low diffraction value in the thin AlN layer.

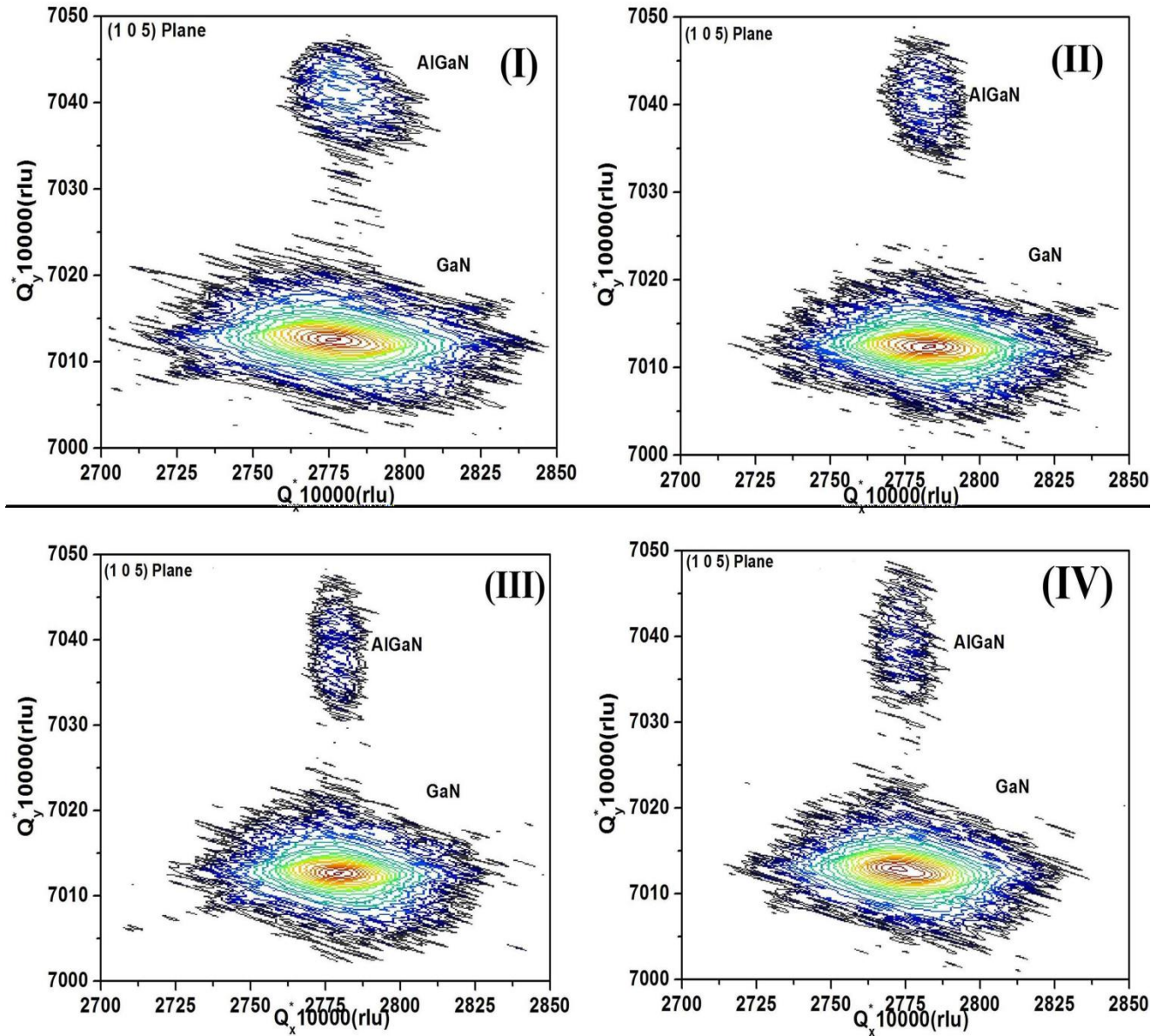


Figure. 5. RSM image of (1 0 5) plane for AlGaIn/GaN heterostructures with sample AlN-IL (I) 0 nm (II) 1 nm (III) 2 nm and (IV) 3 nm

3.3 Photoluminescence and Time resolved Photoluminescence Analysis

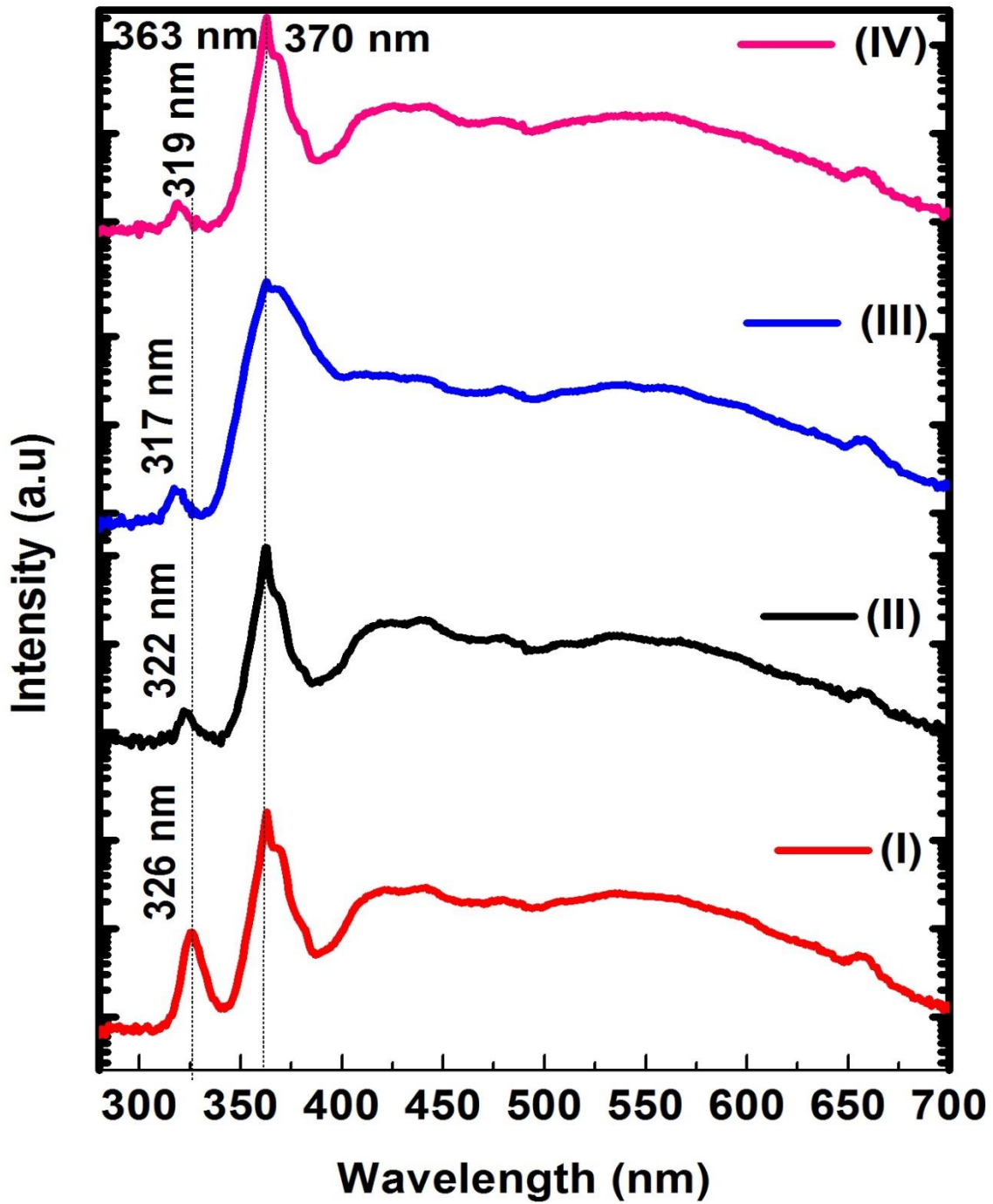


Figure 6. PL spectrum of AlGaN/GaN heterostructures without and with AlN-IL

The RT PL spectra measured in respect of all the samples are shown in Figure 6. The dominant peaks represented by the near-band-edge (NBE) transitions of GaN located at peak energy of ~ 3.41 eV with a pronounced shoulder peaks at 370 nm (3.35 eV). No significant peak shift has been observed in all the grown samples. In this fact, the 3.35 eV peak is accompanying due to the exciton recombination close to the NBE value of GaN and speculates to the 2DEG emission [29, 30]. Another potential interpretation is attributed to the cubic phase inclusions by a wurtzite host lattice, formed as a result of structural defects or stacking Faults (SFs) in GaN [31]. The deconvoluted defect band spectra for sample (I-IV) are shown in figure S3. Here, the blue luminescence (BL) band peak is almost similar to the yellow luminescence (YL) peak in this material. Accordingly, the BL band is possibly assigned to the transitions from deep donor to shallow acceptors [31, 32]. The yellow luminescence band (YL) is associated to the intrinsic defect such as vacancies or interstitial [33-35]. We observed that, the BL and YL intensity is comparatively lower in the sample IV compared to the sample I. Compared to the intensity of the NBE transition; BL and YL is not significant (Less Intensity) in the grown samples.

The PL spectra in respect of AlGaN peaks were observed at 326, 322, 317 and 319 nm for samples I-IV respectively. From the PL data, AlGaN peak was observed to be blue shifted for sample I, II, III. However, a red shift is observed for sample IV due to the compositional fluctuations. It was also noticed that, there were not much considerable changes in the FWHM of AlGaN peaks. As reported in the state of the art [36], the conduction band offset (ΔE_c) between AlGaN and GaN was increased through insertion of an AlN Interlayer. The larger ΔE_c created by the AlN interlayer, could prevent the 2DEG penetrating into the AlGaN layer, which contributes to enrichment in electron concentration. Furthermore, the presence of localized states has a noteworthy impact on the carrier dynamics of TRPL decay times.

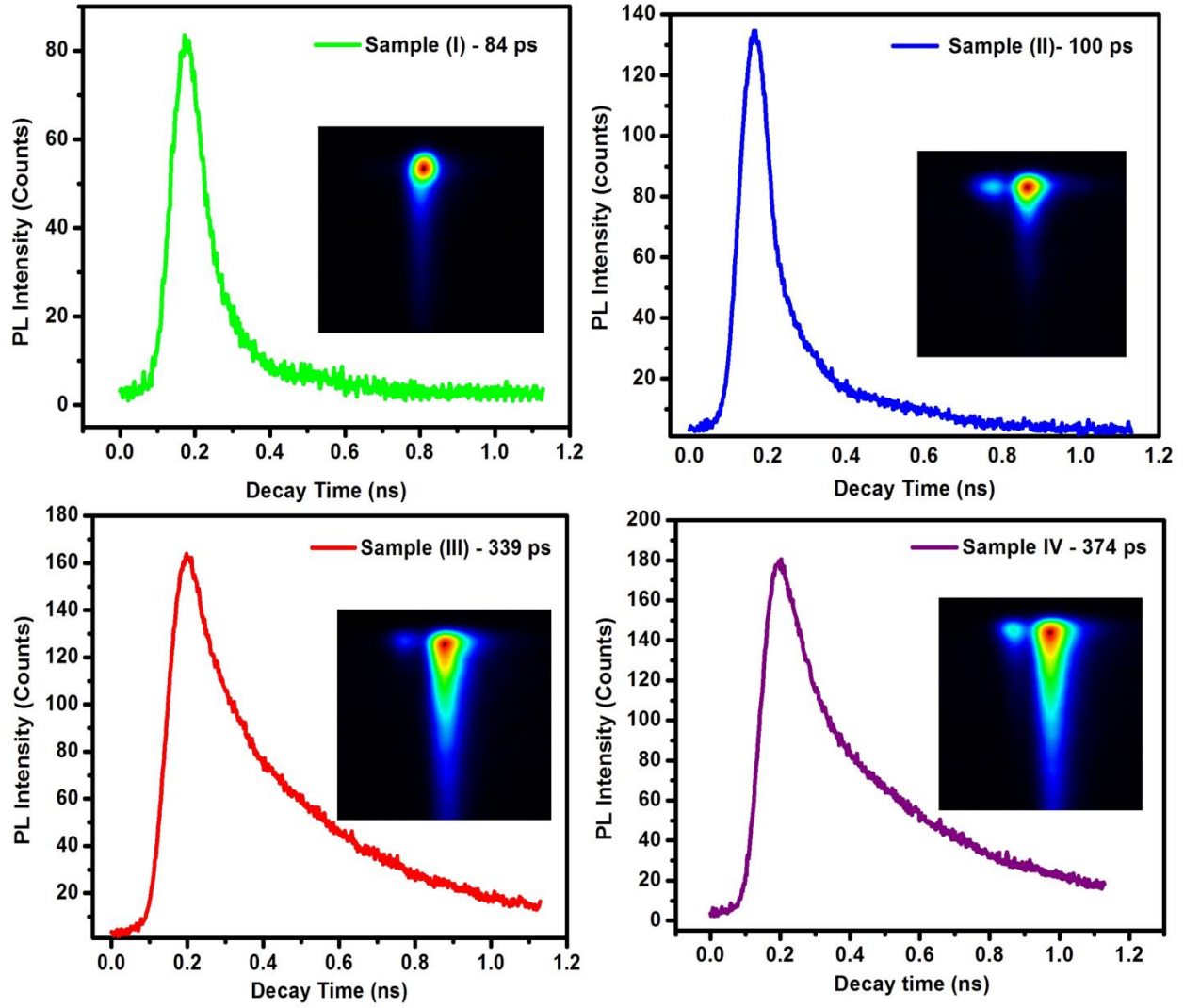


Figure 7. TRPL spectrum of AlGaIn/GaN heterostructures with samples (I) 0 nm (II) 1 nm (III) 2 nm (IV) 3 nm (Insert view-TRPL Streak images)

Figure 7 shows the RT luminescence decay dynamics measured at emission peaks in the spectra (Figure 7) by TRPL spectroscopy. The temporal evolutions of the TRPL spectrum of all four samples are shown in Figure 7 (Insert: i.e., streak images). These streak images observed on “T” shape position. The decay curve fitting for all samples (I-IV) with a biexponential function using the equation (2),

$$I(t) = A_1 \exp\left(-\frac{t}{\tau_1}\right) + A_2 \exp\left(-\frac{t}{\tau_2}\right) \quad (2)$$

Where $I(t)$ is the PL intensity at time t , A_1 and A_2 are the decay parameters and τ_1 and τ_2 are the decay times for a radiative and nonradiative recombination. In the present TRPL measurement profiles, the y-axis represents the number of photons and x-axis is the arrival time [37, 38]. Using the aforesaid fitting procedure, photon decay time estimated is 84, 100, 339 and 374 ps for samples I, II, III, and IV respectively. Sample I, exhibited the lowest decay time and, with the AlN-IL, shows an increase in decay time when increasing the AlN-IL thickness from 0 nm to 3 nm. Sample I and II reveals that the sharp drop in luminescence decay rate can be inferred by a decrease in the radiative recombination rate. It appears that the fast channel is dominating. In the case of sample III and IV, the decay rate is slowing down. It can be inferred by the contribution of more localized excitons with a lower probability to reach non-radiative recombination centers and subsequently achieve longer decay times. It is resultant that slow channeling is starting to pre-dominating recombination process [39, 40].

3.4 Hall Measurement Analysis

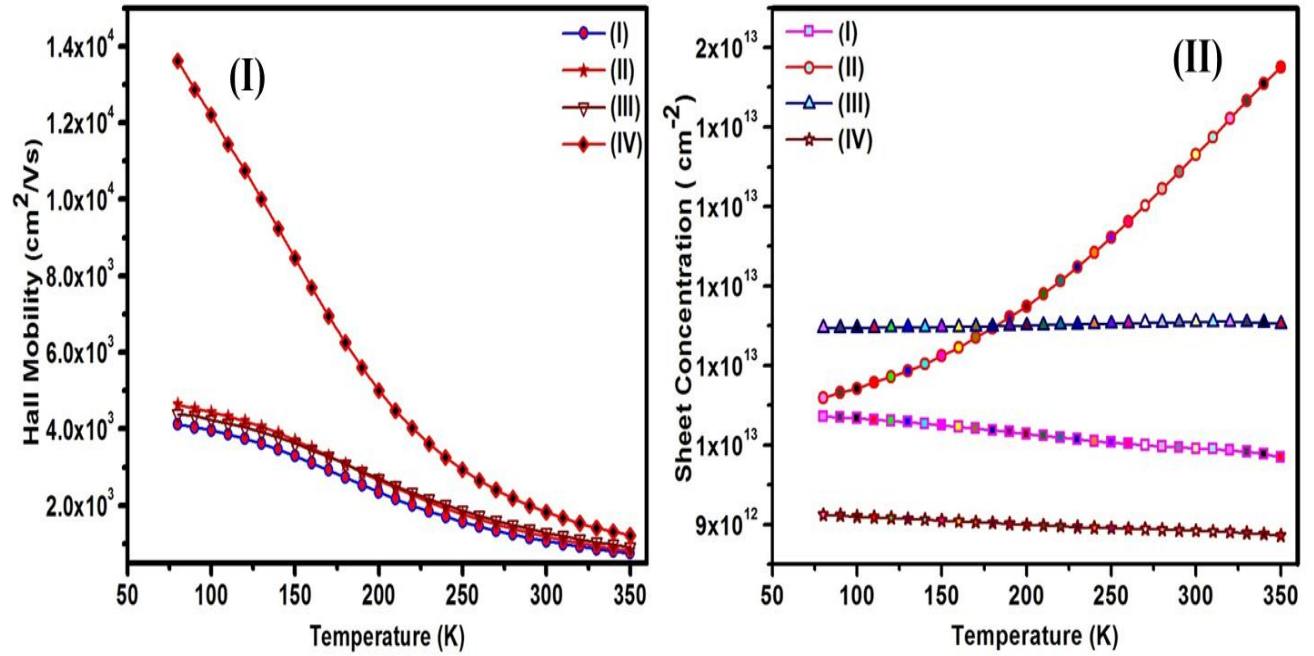


Figure 8. Hall measurements of AlGaIn/GaN heterostructure with and without AlN-ILs corresponding (I) Temperature vs Hall Mobility (II) Temperature vs Sheet Concentration

The electrical characterization in respect of all the samples were performed in a Van der Pauw configuration with tin-indium alloy dots as an ohmic contact. A magnetic field of 0.55 T perpendicular to the sample was used. The temperature dependent sheet concentration and mobility from the measurements can be seen for the AlGaIn/GaN heterostructure with AlN-IL (1 to 3 nm) thickness shown in Figure 8 (I, II). From the figure, it is clear that Hall mobility decreases in all samples when increasing the temperature range from 80 to 350 K. It reveals that the mobility at low temperature (80 K) evidently reduced alloy disorder and/or interface roughness scattering processes [12, 41] through the insertion of AlN-IL between the AlGaIn and GaN layers when compared to the AlGaIn/GaN heterostructures. It is apparent that, the 3 nm AlN-IL in AlGaIn/GaN heterostructures reaches a high mobility and sheet concentration of ~ 13621 cm^2/Vs and $9.1 \times 10^{12}/\text{cm}^2$ with low sheet resistance of 40 ($\pm 1\%$) ohm/sq at 80 K and

$\sim 2000 \text{ cm}^2/\text{Vs}$ and $8.9 \times 10^{12}/\text{cm}^2$ with $280 (\pm 1\%) \text{ ohm/sq}$ at 300 K. The samples without AlN-IL heterostructures had a mobility and sheet concentration of $\sim 4118 \text{ cm}^2/\text{Vs}$ and $1.03 \times 10^{13}/\text{cm}^2$ with sheet resistance $147 (\pm 1\%) \text{ ohm/sq}$ at 80 K and $\sim 1120 \text{ cm}^2/\text{Vs}$ and $9.9 \times 10^{12}/\text{cm}^2$ with sheet resistance $555 (\pm 2\%) \text{ ohm/sq}$ at 300 K. In this case, the AlN-IL thicknesses (1 and 2 nm) with the AlGaIn/GaN heterostructures mobility have slight variations only observed at 300 K and 80 K. When compared to the exclusion of AlN-IL, a high sheet concentration is found for AlN-IL (1 and 2 nm). It is speculated that, at low temperature ranges ($\leq 150 \text{ K}$), the mobilities of AlGaIn/GaN without and with AlN-IL structures could be a temperature independent process [42]. Despite this, above 200 K, the scattering of optical phonons limit the mobility. Our results uphold the theoretical limits with a hall mobility of $\sim 2300 \text{ cm}^2/\text{Vs}$ at 300 K [34, 41, 43]. Also other recent some other report demonstrated 2DEG mobility of about $2000 \text{ cm}^2/(\text{V s})$ at 300 K [15, 44]. The Hall mobility reached up to $800 \text{ cm}^2/\text{Vs}$ at 350 K for samples I to IV. In addition, the 2DEG sheet concentration of samples I, III and IV is almost independent of temperature. In contrast, sample II has a temperature range from 200 K - 350 K, which suggests the involvement of some additional channel conductivity [14]. These results directly indicate that the thin AlN interfacial layer effectively suppresses carrier penetration into the AlGaIn layer by increasing conduction band offset (ΔE_c) and enhances the confinement of the 2DEG in the GaN channel of the AlGaIn/GaN HEMT structures. Based on this information, sample IV (AlN-IL) possess enhanced electrical properties.

4. CONCLUSION

The AlGaIn/GaN heterostructures with AlN Interlayer (IL) (1 to 3 nm) were grown on c-plane sapphire substrates using a MOCVD technique. The effect of AlN-IL thickness on the structural, morphological, optical and electrical properties of AlGaIn/GaN heterostructures were

analyzed using HRXRD, SEM, TEM, AFM, PL, TRPL and Hall measurement studies. The AlGa_N, AlN thickness and Al compositions were estimated through epitaxy smoothfit software. Thickness of AlGa_N, AlN layers were estimated through SEM and TEM. The RSM confirmed that AlGa_N/Ga_N based HEMT structures with AlN-IL are coherently strained. The AlGa_N/AlN (3 nm)/Ga_N heterostructures (sample IV) exhibited an atomically flat, smooth surface, which was verified by AFM analysis. PL results show the effect of AlN-IL thickness dependent band shift in AlGa_N/Ga_N heterostructures, with a high decay time of 374 ps for AlGa_N/Ga_N heterostructures with AlN-IL (3 nm). The insertion of 3 nm AlN-IL on AlGa_N/Ga_N heterostructures achieved a high mobility of 13621 and 2000 cm²/Vs for 80 K and 300 K due to reduced alloy disorder and/or interface roughness scattering processes. Hall mobility was found to be above 800 cm²/Vs at 350K. It is worth noting that the 2DEG hall mobility at 300 K was close to the theoretical limits. This work provides a better understanding relating to the growth of AlGa_N/AlN/Ga_N heterostructure based HEMTs and their structural, morphological, and optical properties, along with the mechanism for their luminescence decay and temperature dependent dominant scattering of the 2DEG mobility and sheet resistance. AlGa_N/Ga_N with AlN-IL based structures can be applied during HEMTs fabrication for the applications in high-temperature and high-power electronic devices.

Acknowledgements

This research work was carried out using Crystal Growth Centre Anna University Laboratories. Manuscript was performed through Aalto University Finland.

References

1. Narang, K., Bag, R.K., Singh, V.K., Pandey, A., Saini, S.K., Khan, R., Arora, A., Padmavati, M.V.G., Tyagi, R. and Singh, R., 2020, Improvement in surface morphology and 2DEG properties of AlGa_N/Ga_N HEMT, *Journal of Alloys and Compounds*, 815, p.152283
2. Çörekçi, S, Öztürk, M K, Akaoglu, B, Çakmak, M, Özçelik, S &Özbay, E 2007, Structural, morphological, and optical properties of AlGa_N/Ga_N heterostructures with AlN buffer and interlayer, *Journal of applied Physics*, vol. 101, no. 12, pp. 123502
3. Tülek, R, Ilgaz, A, Gökden, A, Teke, A, Öztürk, M. K, Kasap, M &Özbay, E 2009, Comparison of the transport properties of high quality AlGa_N/AlN/Ga_N and AlIn_N/AlN/Ga_N two-dimensional electron gas heterostructures, *Journal of Applied Physics*, vol. 105, no. 1, pp. 013707
4. Levinshtein, M E, Ivanov, P A, Khan, M A, Simin, G, Zhang, J Hu, X & Yang, J 2003, Mobility enhancement in AlGa_N/Ga_N metal-oxide-semiconductor heterostructure field effect transistors, *Semiconductor science and technology*, vol. 18, no. 7, pp. 666-669
5. Miyoshi, M, Egawa, T & Ishikawa, H 2006, Study on mobility enhancement in MOVPE-grown AlGa_N/AlN/Ga_N HEMT structures using a thin AlN interfacial layer, *Solid-state electronics*, vol. 50, no. 9, pp. 1515-1521
6. Boles, T., 2018, GaN-on-Silicon—Present capabilities and future directions, In *AIP Conference Proceedings*, Vol. 1934, No. 1, p. 020001
7. Meneghini, M, Bertin, M, Stocco, A, dal Santo, G, Marcon, D, Malinowski, P E &Zanoni, E 2013, Degradation of AlGa_N/Ga_N Schottky diodes on silicon: Role of defects at the AlGa_N/Ga_N interface, *Applied Physics Letters*, vol. 102, no. 16, pp. 163501
8. Choi, S, Heller, E, Dorsey, D, Vetry, R & Graham, S 2013, Analysis of the residual stress distribution in AlGa_N/Ga_N high electron mobility transistors, *Journal of Applied Physics*, vol. 113, no. 9, pp. 093510
9. Manfra, M.J., Weimann, N.G., Hsu, J.W.P., Pfeiffer, L.N., West, K.W., Syed, S., Stormer, H.L., Pan, W., Lang, D.V., Chu, S.N.G. and Kowach, G., 2002. High mobility AlGa_N/Ga_N heterostructures grown by plasma-assisted molecular beam epitaxy on semi-

insulating GaN templates prepared by hydride vapor phase epitaxy, *Journal of applied physics*, 92(1), pp.338-345

10. Zhang, Y., Wang, Z., Xu, S., Bao, W., Zhang, T., Huang, J., Zhang, J. and Hao, Y., 2018. Effects of channel thickness on structure and transport properties of AlGaN/InGaN heterostructures grown by pulsed metal organic chemical vapor deposition, *Materials Research Bulletin*, 105, pp.368-371
11. Tripathy, S., Lin, V.K., Dolmanan, S.B., Tan, J.P., Kajen, R.S., Bera, L.K., Teo, S.L., Kumar, M.K., Arulkumaran, S., Ng, G.I. and Vicknesh, S., 2012. AlGaN/GaN two-dimensional-electron gas heterostructures on 200 mm diameter Si (111), *Applied Physics Letters*, 101(8), p.082110
12. Li, Q., Zhang, J., Meng, L., Chong, J. and Hou, X., 2015. Mobility limitations due to dislocations and interface roughness in AlGaN/AlN/GaN heterostructure, *Journal of Nanomaterials*, 2015, p.8
13. Miyoshi, M., Imanish, A., Ishikawa, H., Egawa, T., Asai, K., Mouri, M., Shibata, T., Tanaka, M. and Oda, O., 2004, October. High performance AlGaN/AlN/GaN HEMTs grown on 100-mm-diameter epitaxial AlN/sapphire templates by MOVPE. In *Compound Semiconductor Integrated Circuit Symposium, IEEE* (pp. 193-196). IEEE
14. Hu, W., Ma, B., Li, D., Narukawa, M., Miyake, H. and Hiramatsu, K., 2009. Mobility enhancement of 2DEG in MOVPE-grown AlGaN/AlN/GaN HEMT structure using vicinal (0 0 0 1) sapphire, *Superlattices and Microstructures*, 46(6), pp.812-816
15. Chen, J.T., Persson, I., Nilsson, D., Hsu, C.W., Palisaitis, J., Forsberg, U., Persson, P.O. and Janzén, E., 2015. Room-temperature mobility above 2200 cm²/Vs of two-dimensional electron gas in a sharp-interface AlGaN/GaN heterostructure, *Applied Physics Letters*, 106(25), p.251601
16. Lee, H.P., Perozek, J., Rosario, L.D. and Bayram, C., 2016. Investigation of AlGaN/GaN high electron mobility transistor structures on 200-mm silicon (111) substrates employing different buffer layer configurations, *Scientific reports*, 6, p.37588
17. Wojtasiak, W., Góralczyk, M., Gryglewski, D., Zając, M., Kucharski, R., Prystawko, P., Piotrowska, A., Ekielski, M., Kamińska, E., Taube, A. and Wzorek, M., 2018. AlGaN/GaN High Electron Mobility Transistors on Semi-Insulating Ammono-GaN Substrates with Regrown Ohmic Contacts, *Micromachines*, 9(11), p.546

18. Jayasakthi, M., Ramesh, R., Arivazhagan, P., Loganathan, R., Prabakaran, K., Balaji, M. and Baskar, K., 2014. Structural and optical characterization of AlGa_N/Ga_N layers, *Journal of Crystal Growth*, 401, pp.527-531
19. Miao, M.S., Weber, J.R. and Van de Walle, C.G., 2010. Oxidation and the origin of the two-dimensional electron gas in AlGa_N/Ga_N heterostructures, *Journal of Applied Physics*, 107(12), p.123713
20. Atmaca, G., Ardali, S., Narin, P., Kutlu, E., Lisesivdin, S.B., Malin, T., Mansurov, V., Zhuravlev, K. and Tiras, E., 2016. Energy relaxation of hot electrons by LO phonon emission in AlGa_N/Al_N/Ga_N heterostructure with in situ Si₃N₄ passivation, *Journal of Alloys and Compounds*, 659, pp.90-94
21. Keller, S., Keller, B.P., Minsky, M.S., Bowers, J.E., Mishra, U.K., DenBaars, S.P. and Seifert, W., 1998. Growth and properties of InGa_N nanoscale islands on Ga_N, *Journal of crystal growth*, 189, pp.29-32
22. Nam, Y., Choi, U., Lee, K., Jang, T., Jung, D. and Nam, O., 2020. Effect of Al_xGa_{1-x}N buffer layer on the structural and electrical properties of AlGa_N/Ga_N/Al_xGa_{1-x}N double heterojunction high electron mobility transistor structures, *Journal of Vacuum Science & Technology B, Nanotechnology and Microelectronics: Materials, Processing, Measurement, and Phenomena*, 38(2), p.022204
23. Manfra, M J, Pfeiffer, L N, West, K W, Stormer, H L, Baldwin, K W, Hsu, J W P & Molnar, R J 2000, High-mobility AlGa_N/Ga_N heterostructures grown by molecular-beam epitaxy on Ga_N templates prepared by hydride vapor phase epitaxy, *Applied Physics Letters*, vol. 77, no. 18, pp. 2888-2890
24. Perozek, J., Lee, H.P., Krishnan, B., Paranjpe, A., Reuter, K.B., Sadana, D.K. and Bayram, C., 2017. Investigation of structural, optical, and electrical characteristics of an AlGa_N/Ga_N high electron mobility transistor structure across a 200 mm Si (1 1 1) substrate, *Journal of Physics D: Applied Physics*, 50(5), p.055103
25. D.K. Bowen, B.K. Tanner, *High Resolution X-ray Diffractometry and Topography*, CRC Press, 2005 p. 58

26. Moram, M.A. and Vickers, M.E., 2009. X-ray diffraction of III-nitrides, Reports on progress in physics, 72(3), p.036502
27. Lazarev, S., Bauer, S., Forghani, K., Barchuk, M., Scholz, F. and Baumbach, T., 2013. High resolution synchrotron X-ray studies of phase separation phenomena and the scaling law for the threading dislocation densities reduction in high quality AlGaIn heterostructure, Journal of Crystal Growth, 370, pp.51-56
28. Cörekçi, S., Oztürk, M.K., Yu, H., Cakmak, M., Ozçelik, S. and Ozbay, E., 2013, Effects of high-temperature AlN buffer on the microstructure of AlGaIn/GaN HEMTs. Физика и техника полупроводников, 47(6), pp.810-814
29. Santana, G., De Melo, O., Aguilar-Hernández, J., Mendoza-Pérez, R., Monroy, B.M., Escamilla-Esquivel, A., López-López, M., De Moure, F., Hernández, L.A. and Contreras-Puente, G., 2013. Photoluminescence study of gallium nitride thin films obtained by infrared close space vapor transport, Materials, 6(3), pp.1050-1060
30. Li, X., Hemmingsson, C., Forsberg, U., Janzén, E. and Pozina, G., 2020. Optical properties of AlGaIn/GaN epitaxial layers grown on different face GaN substrates, Materials Letters, 263, p.127229
31. Reshchikov, M.A. and Morkoç, H., 2005. Luminescence properties of defects in GaN. Journal of applied physics, 97(6), pp.5-19
32. Krishna, S., Aggarwal, N., Gundimeda, A., Sharma, A., Husale, S., Maurya, K.K. and Gupta, G., 2019. Correlation of donor-acceptor pair emission on the performance of GaN-based UV photodetector, Materials Science in Semiconductor Processing, 98, pp.59-64
33. Kucheyev, S.O., Toth, M., Phillips, M.R., Williams, J.S., Jagadish, C. and Li, G., 2002. Chemical origin of the yellow luminescence in GaN, Journal of applied physics, 91(9), pp.5867-5874
34. Pan, L., Dong, X., Li, Z., Luo, W. and Ni, J., 2018. Influence of the AlN nucleation layer on the properties of AlGaIn/GaN heterostructure on Si (1 1 1) substrates, Applied Surface Science, 447, pp.512-517

35. Jing, H.X., Abdullah, C.A.C., Yusoff, M.Z.M., Mahyuddin, A. and Hassan, Z., 2019. Structural and optical properties of AlN/GaN and AlN/AlGa_N/GaN thin films on silicon substrate prepared by plasma assisted molecular beam epitaxy (MBE), *Results in Physics*, 12, pp.1177-1181
36. Wang, C., Wang, X., Hu, G., Wang, J., Li, J. and Wang, Z., 2006. Influence of AlN interfacial layer on electrical properties of high-Al-content Al_{0.45}Ga_{0.55}N/GaN HEMT structure, *Applied Surface Science*, 253(2), pp.762-765
37. Fan, S., Qin, Z., He, C., Hou, M., Wang, X., Shen, B., Li, W., Wang, W., Mao, D., Jin, P. and Yan, J., 2013. Optical investigation of strong exciton localization in high Al composition Al_xGa_{1-x}N alloys, *Optics Express*, 21(21), pp.24497-24503
38. Onuma, T., Chichibu, S.F., Uedono, A., Sota, T., Cantu, P., Katona, T.M., Keading, J.F., Keller, S., Mishra, U.K., Nakamura, S. and DenBaars, S.P., 2004. Radiative and nonradiative processes in strain-free Al_xGa_{1-x}N films studied by time-resolved photoluminescence and positron annihilation techniques. *Journal of applied physics*, 95(5), pp.2495-2504
39. Ochalski, T.J., Grzegorzczak, A., Rudzinski, M., Larsen, P.K., Holtz, P.O., Bergman, P. and Paskov, P.P., 2005. Optical study of AlGa_N/GaN based HEMT structures grown on sapphire and SiC, *physica status solidi (a)*, 202(7), pp.1300-1307
40. Mickevičius, J., Tamulaitis, G., Kuokštis, E., Liu, K., Shur, M.S., Zhang, J.P. and Gaska, R., 2007. Well-width-dependent carrier lifetime in AlGa_N/AlGa_N quantum wells, *Applied physics letters*, 90(13), p.131907
41. Forsberg, U., Lundskog, A., Kakanakova-Georgieva, A., Ciechonski, R. and Janzén, E., 2009. Improved hot-wall MOCVD growth of highly uniform AlGa_N/GaN/HEMT structures, *Journal of Crystal Growth*, 311(10), pp.3007-3010
42. Kaun, S.W., Burke, P.G., Hoi Wong, M., Kyle, E.C., Mishra, U.K. and Speck, J.S., 2012. Effect of dislocations on electron mobility in AlGa_N/GaN and AlGa_N/AlN/GaN heterostructures, *Applied Physics Letters*, 101(26), p.262102

43. Skierbiszewski, C., 2005. From high electron mobility GaN/AlGaN heterostructures to blue-violet InGaN laser diodes, perspectives of MBE for nitride optoelectronics. ACTA PHYSICA POLONICA SERIES A, 108(4), p.635
44. Xu, X., Zhong, J., So, H., Norvilas, A., Sommerhalter, C., Senesky, D.G. and Tang, M., 2016. Wafer-level MOCVD growth of AlGaIn/GaN-on-Si HEMT structures with ultra-high room temperature 2DEG mobility, AIP Advances, 6(11), p.115016